6.

Digital Instrument Response Correction for the Force-Balance Accelerometer

Elena I. Novikova and M. D. Trifunac, M.EERI

Correction for the instrument response of acceleration records obtained by force balance accelerometers (FBA) is necessary (a) to eliminate phase distortion at high frequencies, and (b) to broaden the useful frequency band up to, and beyond, the corner frequency of the system. The proposed algorithm contains operations in the time domain only and can be applied to any digitized record obtained from a FBA with known characteristics. The adequacy of the procedure depends on the accuracy of the information on the transducer's constants: damping ratio and natural frequency. An appropriate testing procedure is also presented.

INTRODUCTION

The need for carefully processed strong motion records in buildings is increasing. The studies of structural response, elastic wave propagation, and of soil repose all require accurate information about the amplitude and the phase of motion throughout a wide range of frequencies. However, the records obtained by most experimental procedures contain distortions which are caused by the physical properties of the transducers and the recording devices. If the record is analog, it should be digitized before it can be used in analysis. The process of digitization introduces some noise. The study of this noise gives information on the frequency band where the data has good signal to noise ratio. Some recording instruments produce digital output. This means that some analog to digital (A-D) converter is included into the measuring system, and in this case it's characteristics must be studied to account for the possible distortions it introduces into the signal being recorded. Thus, what we see as a digital "record" is not the actual time-history of the acceleration (velocity or displacement), but the response of the transducer and the recording device to the input motion. Historically, investigators were concerned mainly with the amplitude of motion (not the phase), and were trying to design the transducers and the entire measuring systems in such a way that their amplification in some frequency range can be approximated by a constant. However, it is not possible to make this amplification exactly equal to a constant, and it is even more difficult to control simultaneously the phase of the responses. This is why correction of the output of the recording system is needed. This correction "translates" the response of the device

Department of Civil Eng., University of Southern California, Los Angeles, CA 90089

back to the original excitation that caused the recorded response. Good instrument correction allows one to reconstruct both amplitudes and phases of motion well beyond the frequency range where the amplification of the instrument can be approximated by a constant (Trifunac 1972, Trifunac and Lee 1974). This paper deals with such a correction for the widely used force-balance accelerometer.

Force-balance transducers differ from other types of transducers by having an electrical feedback loop (Fig. 1) designed to keep the sensing mass in equilibrium position. This is achieved by applying a balancing force, equal in magnitude and opposite in direction to the "outside" force produced by the acceleration being measured. An electrical pick-up is used to sense the relative mass motion, its output is amplified, and the required feedback current is generated.

Force-balance transducers were studied by many investigators (Amini and Trifunac, 1985; Amini et al. 1991; Hudson, 1979; Neubert, 1975; Norton, 1969; Oliver, 1971) and it was shown that there are certain advantages in using this system, compared to the conventional open-loop devices. Those advantages are: 1) broadening the frequency range of the measurement, 2) the possibility to alter the natural frequency and damping of the transducer by changing the electrical constants (utilizing the fact that the mechanical damping is negligible), and 3) significant reduction of cross-axis sensitivity (due to practically zero relative mass motion) (Wong and Trifunac, 1977). These factors and the relative simplicity of the transducer lead to the wide use of the force-balance transducers in dynamic measurements of ground and structural motions in earthquake engineering and in many other related fields.

For low frequency applications, records from force balance transducers can be interpreted as being recorded by a single degree-of-freedom viciously damped system. However, in more detailed and broader band applications (e.g., in structural identification), more accurate and high frequency data may be required. Also, when structural components experience non-linear deformation, "brittle" failure mode of concrete in compression can produce frequencies in excess of 100 Hz (Kojić et al., 1984), and to interpret these, and to use the recordings of structural response which include such high frequency signals, it is necessary to use more detailed corrections for the instrument response. In this paper, such a correction algorithm is presented.

TRANSFER FUNCTION OF A FBA

A general scheme of a force balanced accelerometer is presented in Fig. 1. The acceleration to be measured is applied along the axial direction of the transducer. Relative displacement of the transducer mass M caused by the applied acceleration is sensed by a variable capacitance with sensitivity D(volts/meter) and converted into a voltage output. This voltage is sent to an amplifier of gain k and a velocity-sensing pick-up, or to a phase-advancing network with transfer function $(1 + qd/dt)$. The output current is fed into a force generator with the amplitude modified by the generator constant $G(N/\mathrm{Amp})$. The force produced completes the feed-back loop balancing the inertia force of the transducer mass caused by the acceleration, so that the mass M remains stationary relative to the instrument housing.

The work presented here deals with one type from the family of Force Balance Accelerometers exemplified by FBA-1 (manufactured by Kinemetrics, Amini and Trifunac, 1985) and RJL-1 (manufactured by the Institute of Engineering Mechanics, SSB in Harbin China, Amini et al., 1991). In contrast to the general scheme shown in Fig. 1 (where the output voltage is proportional to the displacement and velocity of the moving mass), their output is proportional to the displacement alone

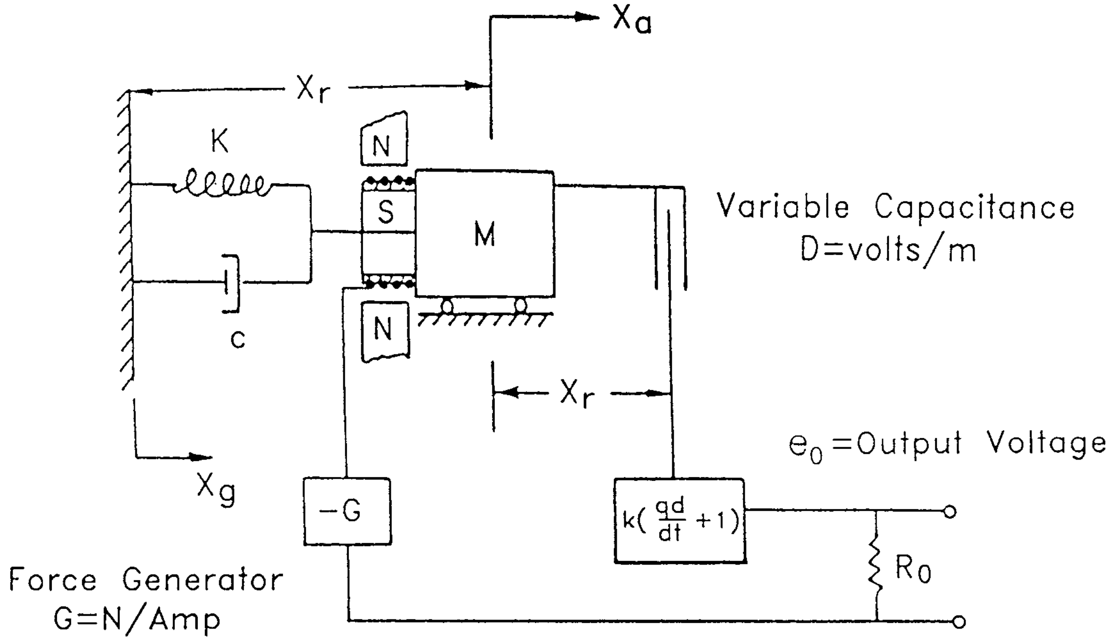

Figure 1. Force Balance Accelerometer Block Diagram. X_g is the absolute ground displacement, X_a stands for the absolute displacement of the mass M and X_r is the relative displacement of the mass.

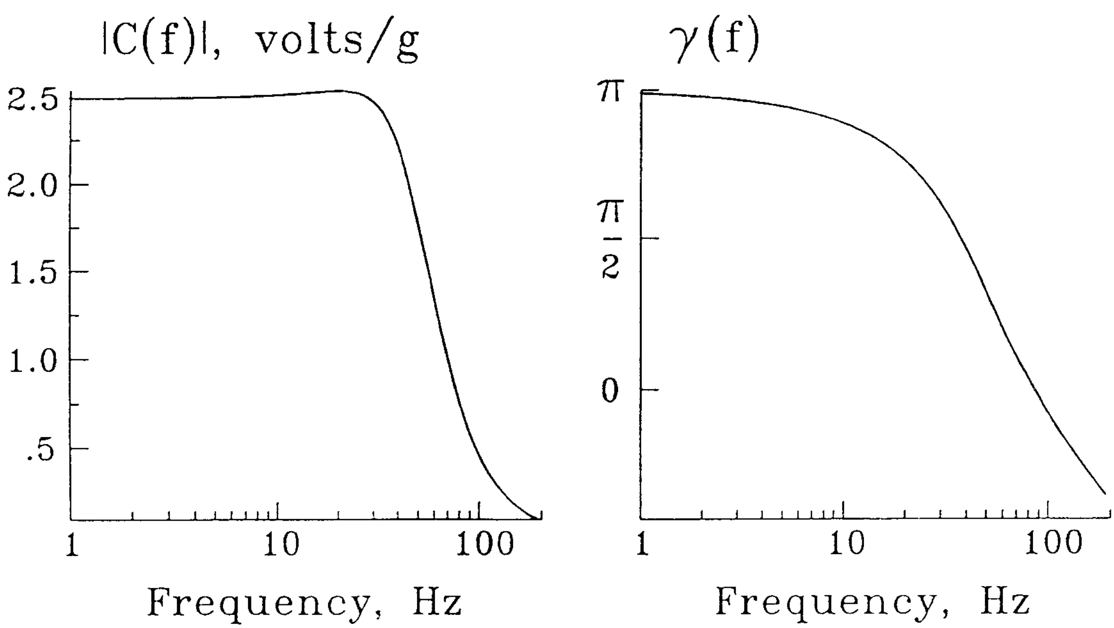

Figure 2. The modulus $|C(f)|$ (left) and the phase shift $\gamma(f)$ (right) of the FBA-1 transfer function.

$(q = 0)$. This transducer was studied in detail by Amini and Trifunac (1985), who presented its transfer function in the Laplace transform domain (s-domain) as follows

$$e_0 = \frac{R_{10}+R_9}{R_{10}} \cdot \frac{R_h+R_8}{R_8} \cdot \frac{1}{1+R_{11}C_3 s} \cdot \frac{1}{1+R_6 C_2 s} \cdot \frac{-D\ddot{x}(s)\cdot A^*}{s^2+2\omega_n \xi s+\omega_n^2}. \tag{1}$$

Here e_0 is the output voltage, $\ddot{x}(s)$ stands for the input acceleration,

$$A^* = \frac{M}{M+KC_0L_c+KC_0R_cC_2R_6+cC_0R_c+cC_2R_6},$$

$$2\xi\omega_n = \frac{c+KC_0R_c+KC_2R_6+GDC^*\frac{R_h+R_8}{R_8}}{M+KC_0L_c+KC_0R_cC_2R_6+cC_0R_c+cC_2R_c}$$

and

$$\omega_n^2 = \frac{K+GD\frac{R_0+R_h+R_8}{R_0R_8}}{M+KC_0L_c+KC_0R_cC_2R_6+cC_0R_c+cC_2R_c},$$

where c stands for the mechanical damping, C^* is the series combination of capacitors C_6 and C_7 and R_i are the resistances, L_i are inductances and C_i the capacitors in the system logic (Amini and Trifunac, 1985). This device is equivalent to a combination of a single degree of freedom system with corner frequency ω_n and critical damping ratio ξ, and two low-pass linear filters with corner frequencies $\omega_1 = 2\pi f_1 = (R_{11}C_3)^{-1}$ and $\omega_2 = 2\pi f_2 = (R_6C_2)^{-1}$ respectively (Amini et al., 1991). Typical values of the electrical constants involved are such that f_1 and f_2 are relatively high. In the FBA studied by Amini and Trifunac (1985), the numerical values of f_1 and f_2 are 310 Hz and 160 Hz respectively. This allows one to consider the following approximation of Eq. (1) for low frequencies $(f << \min(f_1, f_2))$:

$$e_0 = D\frac{R_{10}+R_9}{R_{10}} \cdot \frac{R_h+R_8}{R_8} \cdot \frac{-\ddot{x}(s)}{s^2+2\omega_n\xi s+\omega_n^2}, \tag{2}$$

where

$$2\xi\omega_n = \frac{DGC^*}{M} \cdot \frac{R_h+R_8}{R_8}$$

and

$$\omega_n^2 = \frac{DG}{M} \cdot \frac{R_0+R_h+R_8}{R_0R_8}.$$

Equation (2) corresponds to the conditions when the frequencies of the process being measures are so low that the two linear low-pass filters can be neglected.

Manufactures and some users of the FBA system often characterize it only by the natural frequency, ω_n, and critical damping ratio, ξ, based on its representation as a single degree of freedom system, i.e. as being described by Eq. (2). For the particular transducer studied by Amini and Trifunac (1985), these constants were $f_n = \omega_n/2\pi = 51.2$ Hz and $\xi = 0.65$. This representation is adequate for sufficiently low frequencies. However, both low-pass filters influence the transfer function of the transducer even for these low frequencies, resulting in shifting the "effective" values of f_n and ξ. A shaking table test performed by Amini and Trifunac (1985) gave for the same device constants $f_n = 47$ Hz and $\xi = 0.62$, by fitting the experimental data to Eq. (1).

Utilizing their results and the nominal value of amplification of the system (2.5 volts per 1g of acceleration, where g = 9.81 m/sec^2), Eq. (1) can be rewritten into the frequency domain (by setting $s = i\omega$) as:

$$e_0 = C(\omega) \cdot \ddot{x}(\omega),$$

where $C(\omega)$ represents the transfer function of the system:

$$C(\omega) = \frac{1}{1 + i\omega R_{11} C_3} \cdot \frac{1}{1 + i\omega R_6 C_2} \cdot \frac{-\rho\omega_n^2}{-\omega^2 + 2i\omega\omega_n\xi + \omega_n^2}. \tag{3}$$

In this example $\rho = 2.5$ volts/g, $\omega_n = 2\pi \cdot 47$ Hz, and $\xi = 0.62$, and the other constants can be taken from Amini and Trifunac (1985). The graph of the transfer function (3) in terms of frequency $(f = \omega/2\pi)$, $C(f) = |C(f)|e^{i\gamma(f)}$ is presented, in Fig. 2. As can be seen from this figure, this FBA produces a signal which is proportional to the acceleration being measured for the frequencies less than $\sim$ 30 Hz. For $f \geq 30$ Hz, the gain of the device gradually rolls off, and then (for $f > 35 \div 40$ Hz) decreases as a power function. The phase diagram indicates appreciable phase shift for all frequencies.

Modern studies of structural vibrations, wave propagation phenomena and soil-structure interaction problems require accurate information about the phase of the recorded motion. The further broadening of the useful frequency range is also of considerable interest. These considerations lead us to the conclusion that the instrument correction of the output from the force-balance accelerometer is necessary.

AN ALGORITHM FOR CORRECTION OF THE INSTRUMENT RESPONSE

The proposed algorithm is based on the same principles as in several previous studies (Trifunac, 1972; Novikova and Trifunac, 1991). The procedure uses the differential equation of the system and includes digital filtering in the time domain only.

The forth order differential equation of a force-balance accelerometer (FBA) can be obtained by rewriting Eq. (3) in time domain:

$$\begin{aligned} &\ddddot{e}_0[R_{11}C_3R_6C_2] + \dddot{e}_0[2\omega_n\xi R_{11}C_3R_6C_2 + R_{11}C_3 + R_6C_2] + \\ &+ \ddot{e}_0[1 + 2\omega_n\xi(R_{11}C_3 + R_6C_2) + \omega_n^2 R_{11}C_3R_6C_2] + \\ &+ \dot{e}_0[2\omega_n\xi + \omega_n^2(R_{11}C_3 + R_6C_2)] + e_0 \cdot \omega_n^2 = -\rho\omega_n^2\ddot{x} \, , \end{aligned} \tag{4}$$

where each dot over e_0 designates one differentiation with respect to time. As before, e_0 designates the output voltage and $\ddot{x}$ is the absolute acceleration being measured. It should be emphasized that the adequacy of the description of a FBA by Eq. (4) depends on the accuracy of the information about all the constants involved in this equation. As it was pointed out by Amini and Trifunac (1985), ω_n and ξ, supplied by the manufacturers, often correspond to Eq. (2) and are good for low frequency representation only. Special procedures should be developed to measure ω_n and ξ which can go along with Eq. (1) (and, correspondingly, with Eq. (4)) to describe the system in the high-frequency range as well as in the low-frequency range.

We assume here that the galvanometer (or other recording device) attached to FBA has infinite impedance, and, consequently, there is no feedback from the recording system to the transducer. This means that the system of two devices involved in the measurement is uncoupled, and Eq. (4) can be analyzed alone. If this is not the case, the whole procedure can be changed to accommodate coupling (Novikova and Trifunac, 1991).

Having the output voltage e_0 as a function of time, all the four derivatives of e_0, involved in Eq. (4), can be obtained by numerical differentiation. However, prior to this, the frequency band of interest should be identified. This can be accomplished in the manner similar to what was used by Lee and Trifunac (1979, 1984). Comparison of the Fourier spectra of the "standard noise" and signal (plus noise contained in it) can indicate the frequency band where signal to noise ratio remains higher than a prescribed value. (By "standard noise" we mean the average digitization noise, typical for the records being processed.) We are particularly interested in the higher limit of the frequency band, f_+, as this value is going to govern the instrument correction procedure. Given the output voltage e_0, we will try to reconstruct "exact" acceleration of the moving point for all frequencies lower than f_+.

Each numerical differentiation should be followed by a low-pass filtering with corner frequency f_+. It is easy to combine both procedures in one filter. However, as it often happens (Hamming, 1983), by forcing the filter to do two tasks simultaneously, one may not get either of them done properly. Thus we separate the differentiation and the low-pass filtering.

The differentiating filter used has the pulse response (Novikova and Trifunac, 1991):

$$\mathrm{w}_{\pm k} = \frac{\pm 1}{k}\left\{\frac{\sin(\pi k/N)}{(\pi k/N)}\right\}^2, \quad \mathrm{w}_0 = 0, \quad k = 1, 2, ..., N. \tag{5}$$

Here w_k are filter weights and N is equal to the half length of the filter and depends on the accuracy the filter has to achieve. Factor in $\{\cdot\}^2$ represents squared Lanczos coefficients and it was introduced to reduce the Gibb's phenomenon (Hamming, 1983). The antisymmetry of the filter provides for the "exact" behavior of the phase (it is not distorted with respect to the theoretical $\frac{\pi}{2}$ shift appearing during differentiation). The transfer function of the filter in Eq. (5) is plotted in Fig. 3 against the dimensionless frequency $\overline{f} = f/f_{\mathrm{sampling}}$, where f_{sampling} is the frequency of sampling. Nyquist frequency in these units is $\overline{f}_N = 0.5$.

Two types of filters were utilized for low-pass filtering. When $\overline{f}_+ = f_+/f_{\mathrm{sampling}} \geq 0.25$ (in dimensionless units), numerical approximation of the step function (in frequency domain) with corner frequency $\overline{f}_+$ gives the following expression for the pulse response of the "sharp" filter:

$$\mathrm{w}_{\pm k} = \frac{1}{\pi k}(\sin(2\pi \overline{f}_+ k)) \cdot \mathrm{w}_k^*, \quad \mathrm{w}_0 = 2\overline{f}_+, \quad k = 1, 2, ..., N. \tag{6}$$

Here w_k are the weights of the filter, N is it's half-length and w_k^* represents Webber's windowing, which can be approximated by two cubic parabolae (Cappellini et

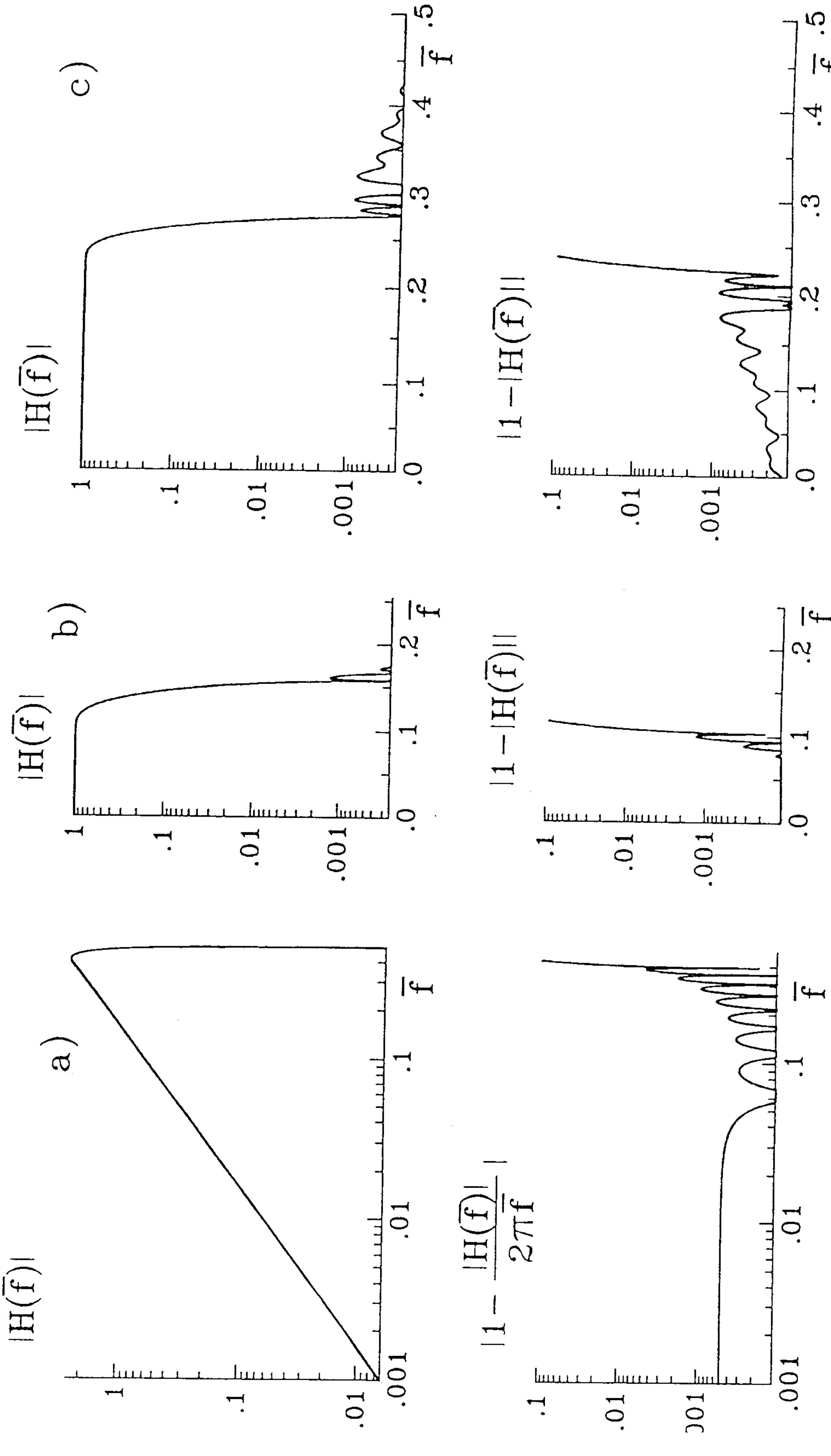

Figure 3. The moduldi of the transfer functions (top) and of their relative errors (bottom) as functions of dimensionless frequency $\overline{f}$. a) differentiating filter, b) Ormsby filter, c) "sharp" filter.

al., 1978). Transfer function of the filter in Eq. (6) is plotted on Fig. 3. This filter works well for high cut-off $\overline{f}_+$, but requires large number of points (N) for low cut-off. Failure to increase the filter length results in poor control of the shape of it's transfer function.

Ormsby filter is used as a low-pass filter for the case when $\overline{f}_+ < 0.25$. Instead of trying to model the step function, as the "sharp" filter in Eq. (6) does, Ormsby filter approximates, by short finite series, the transfer function which linearly decreases from the cut-off frequency $\overline{\omega}_c = 2\pi\overline{f}_+$ to the roll-off frequency $\overline{\omega}_s$, and is 1 when $\overline{\omega} < \overline{\omega}_c$ and 0 when $\overline{\omega} > \overline{\omega}_s$ (here $\overline{\omega} = \omega/2\pi f_{\text{sampling}}$). This shape is more "natural" for the transfer function of a digital low-pass filter, and this allows one to reduce the number of filter weights required to obtain sufficient accuracy. Pulse response of the Ormsby filter with von Hann windowing is described by the following filter weights w_k:

$$\mathrm{w}_{\pm k} = \frac{\cos(\overline{\omega}_c k) - \cos(\overline{\omega}_s k)}{2\pi^2(\overline{\omega}_s - \overline{\omega}_c)k^2} \cdot \left\{\frac{1}{2}\left(1 + \cos\left(\frac{k\pi}{N}\right)\right)\right\}, \tag{7}$$
$$\mathrm{w}_0 = \frac{\overline{\omega}_s + \overline{\omega}_c}{4\pi^2}, \qquad k = 1, 2, ..., N.$$

The roll-off frequency, $\overline{\omega}_s$, can be obtained by the comparison of the requirements for the length of the filter $2N+1$ and the "sharpening" of it (Novikova and Trifunac, 1991). Transfer function of the filter in Eq. (7) is presented in Fig. 3. Both "sharp" (Eq. (6)) and Ormsby (Eq. (7)) low-pass filters used are symmetric and this provides an exact phase representation, which is essential in earthquake engineering data processing (Lee and Trifunac, 1984).

Having defined the filters in Eq. (5) through Eq. (7), one can proceed with numerical differentiation (followed by low-pass filtering) of the output signal e_0. After calculating all four derivatives of the output voltage, the "exact" acceleration of the moving point can be reconstructed by substitution of all the functions obtained ($\dot{e}_0, \ddot{e}_0, \dddot{e}_0$ and $\ddddot{e}_0$) together with e_0 into the differential equation of the transducer, Eq. (4).

CASE STUDY

A typical strong motion accelerogram (Lee and Trifunac, 1987) was used in the testing procedure. This was the vertical component of the record obtained during the Imperial Valley earthquake in California, on October 15, 1979, at the epicentral distance of 27 km, by USGS, at El Centro Array Station #8. As all the records in EQINFOS files, (Lee and Trifunac, 1987), this record has sampling rate of 50 samples per second (sps). This record does not have frequencies high enough for the purpose of testing the instrument correction procedure for a FBA. To use this record, it was "shrunk" 5 times along the time axis and, therefore, it's spectrum was shifted towards high frequencies so that the Nyquist frequency became $25 \cdot 5 = 125$ Hz (sampling 250 sps). Thus shrunk record of the total length to 7.5 sec was adopted as "exact ground acceleration." The first "3 seconds" of this record are presented in Fig. 4 along with the Fourier spectrum of the whole "shrunk" record.

Given $\ddot{x}(t)$, Eq. (4) can be solved for e_0 by Runge-Kutta (fourth order) integration. This procedure numerically simulates the work of a FBA during the recording

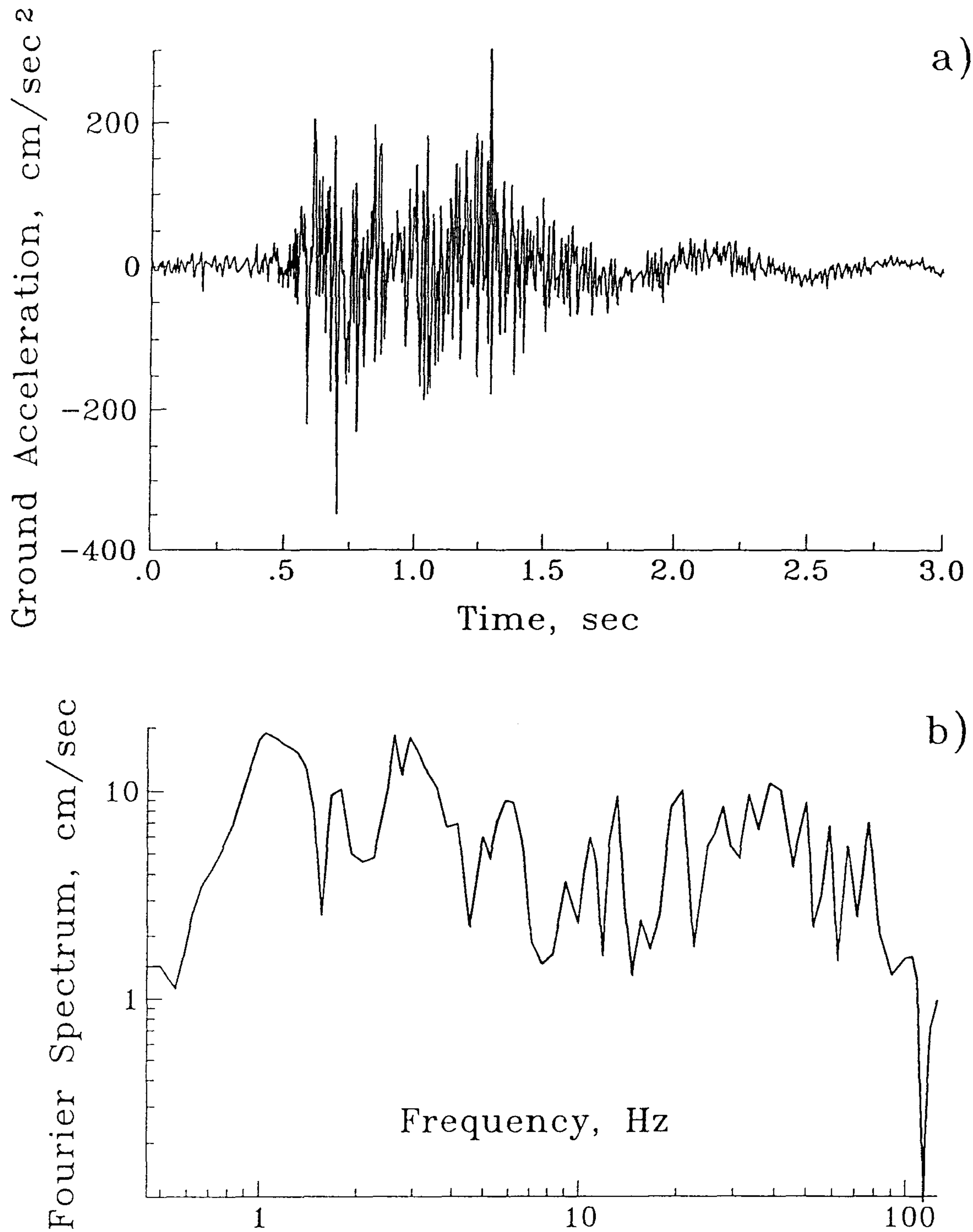

Figure 4. Five times "shrunk" vertical component of the record obtained during the Imperial Valley earthquake in California, on 10/15/79 at the epicentral distance 27 km. a) first 3 sec of the time history, b) Fourier spectrum of the whole record (7.5 sec).

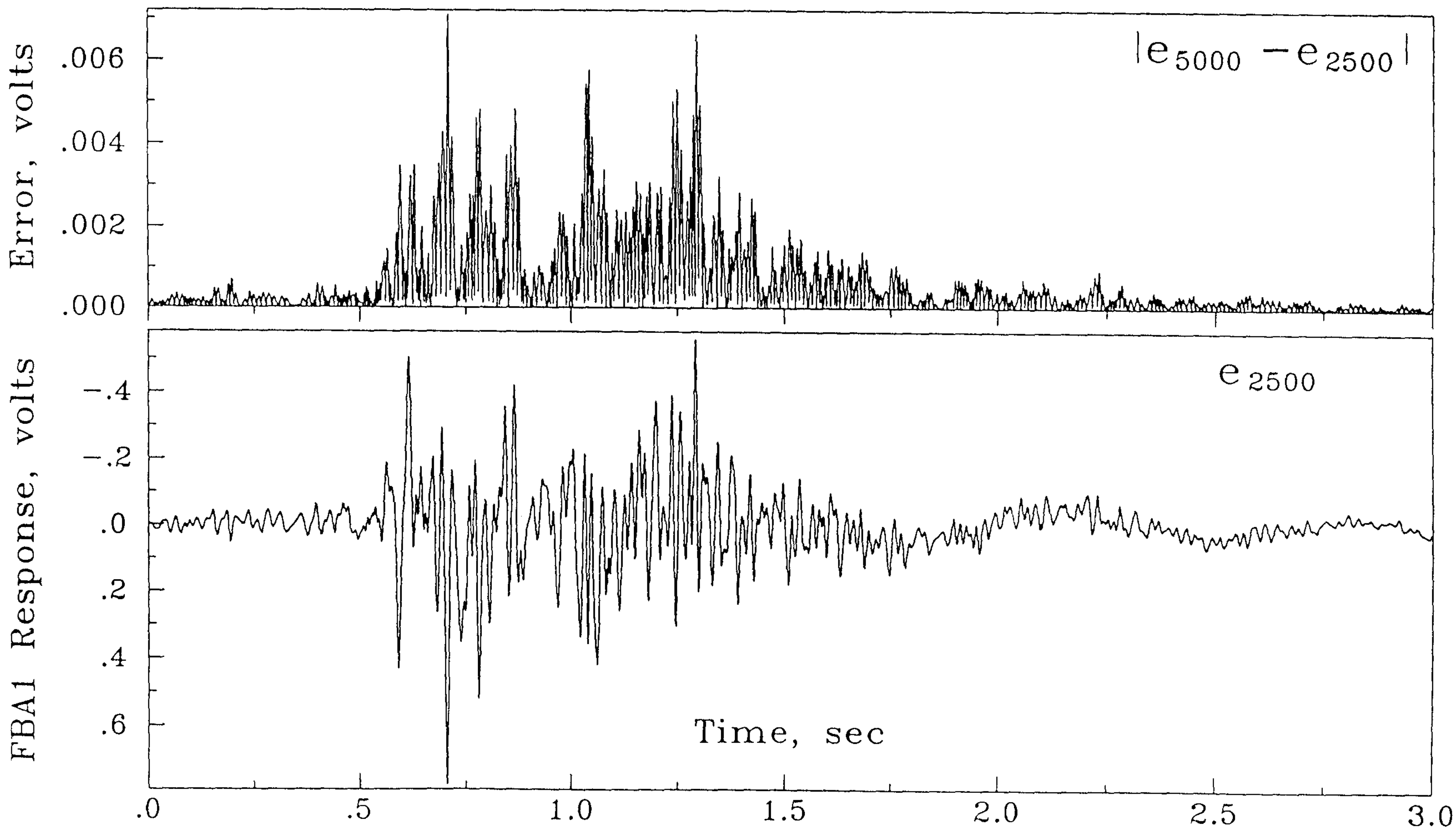

Figure 5. "Recording" of the excitation from Fig. 4 by the mathematical model of FBA-1 - the output of the Runge-Kutta integration, with 2500 sps sampling rate (bottom) and the estimation of the absolute error of this integration (top).

process. So "recorded" ground motion then has to be corrected for the instrument response. The corrected accelerogram can be compared with the exact acceleration which served as an input to the mathematical model of a FBA (Runge-Kutta integration of Eq. (4)). If the comparison shows that the reconstructed record almost coincides with the exact acceleration, one can conclude that the proposed algorithm for instrument correction is able to perform its task. Prior to integration, the record has to be interpolated (Novikova and Trifunac, 1991) to higher sampling rate, so that the Runge-Kutta procedure will not contribute additional errors.

To estimate the errors of the integration, one can consider the following test. First, interpolate the record from 250 sps to, say, 2500 sps and carry out the Runge-Kutta integration. Call this output e_{2500}. Second, obtain e_{5000} - the output of the same procedure for the sampling rate increased to 5000 sps. Now the modulus of the difference between these two outputs $|e_{5000} - e_{2500}|$ can serve as an estimate of the absolute error of e_{2500} due to numerical integration. Fig. 5 shows e_{2500} (t) and $|e_{5000}(t) - e_{2500}(t)|$. As one can see, the average error of the Runge-Kutta fourth order integration is about 1% for this record. The Y-axis is flipped in Fig. 5 (bottom) to make the comparison between the "exact" (Fig. 4) and the "recorded" (Fig. 5 bottom) accelerations easier (recalling Fig. 2, one can notice π-lag in the transfer function of the device). This comparison shows high distortion of the record during the "recording process."

Next step in the testing procedure is to perform the instrument correction on the record, via the mathematical model of a FBA. Instrument correction does not require so high sampling rate as Runge-Kutta does, so the e_{5000} can be decimated to say, 1000 sps (recall that the assumed input motion has frequency band from essentially zero to 125 Hz). Prior to decimation, e_{5000} has to be low-pass filtered with corner frequency 500 Hz = 0.5·1000 Hz to avoid aliasing. Fig. 6 shows the difference between the exact acceleration $\ddot{x}$ and the output of "Runge-Kutta → Instrument-Correction" testing process (called $\ddot{x}_{icr}$). The two functions, $\ddot{x}(t)$ and $\ddot{x}_{\text{icr}}(t)$, cannot be distinguished by eye in this scale. The average error of $\ddot{x}_{icr}$ is about 5%. Recalling the value of the error introduced during integration, one can conclude that $|\ddot{x} - \ddot{x}_{icr}|$ comes predominantly from the instrument correction.

Fig. 7a shows a small portion of the same record but with a larger scale. The exact appropriately scaled "recorded" and the reconstructed acceleration are plotted together for the purpose of comparison. The phase shift of 180 degrees for the "recorded" time history was taken into account in Fig. 7. However, one can notice appreciable additional phase shift introduced by the device. Fig. 7b allows one to check the performance of the instrument correction algorithm in the frequency domain. As one can see, the ground acceleration can be adequately reconstructed up to frequencies which are far beyond the corner frequency of the recording device.

CONCLUSIONS

The correction of the records obtained by a FBA is necessary for reconstruction of the true phase in the motion, and also allows one to broaden the frequency range available for the analysis. This correction can be performed in the time domain by solving the forth order differential equation of the transducer. The accuracy of the procedures considered here is very good in both time and frequency domain. The quality of the whole process is limited by the accuracy of the information on the constants of the device (natural period and damping). Another assumption made is that the galvanometer used in the recording has infinite impedance.

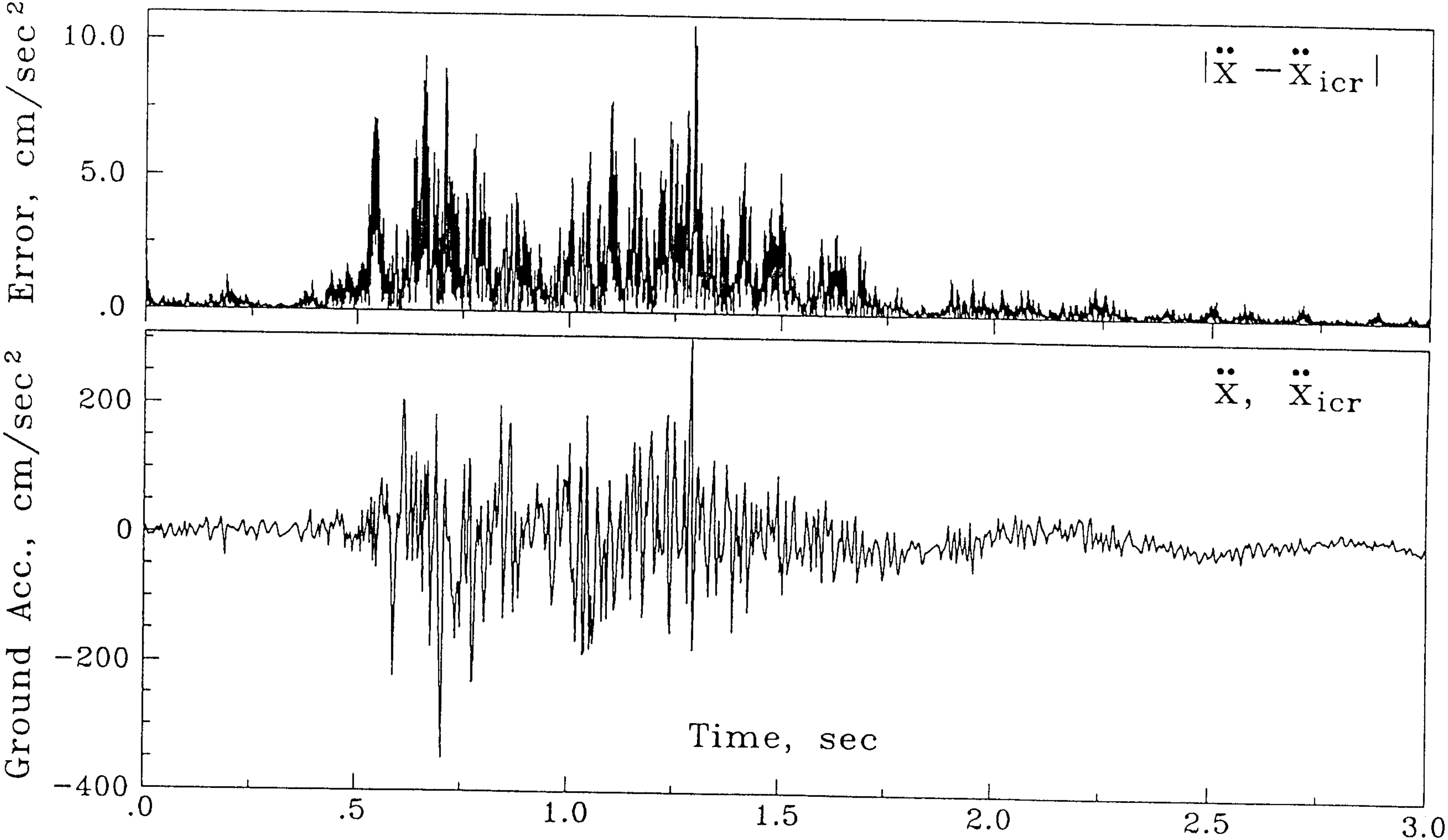

Figure 6. The exact ground acceleration $\ddot{x}$ and the reconstructed acceleration $\ddot{x}_{icr}$ are shown in the bottom (lines coincide). Absolute global error of instrument correction (the difference $|\ddot{x} - \ddot{x}_{icr}|$) is shown on top.

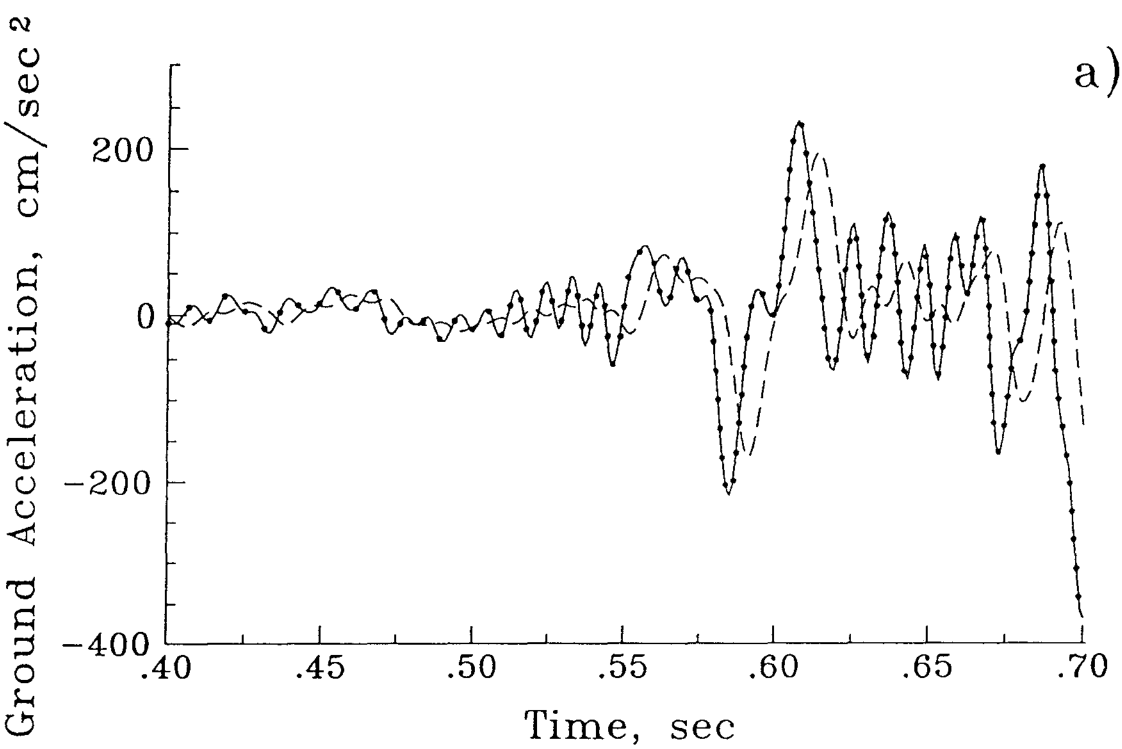

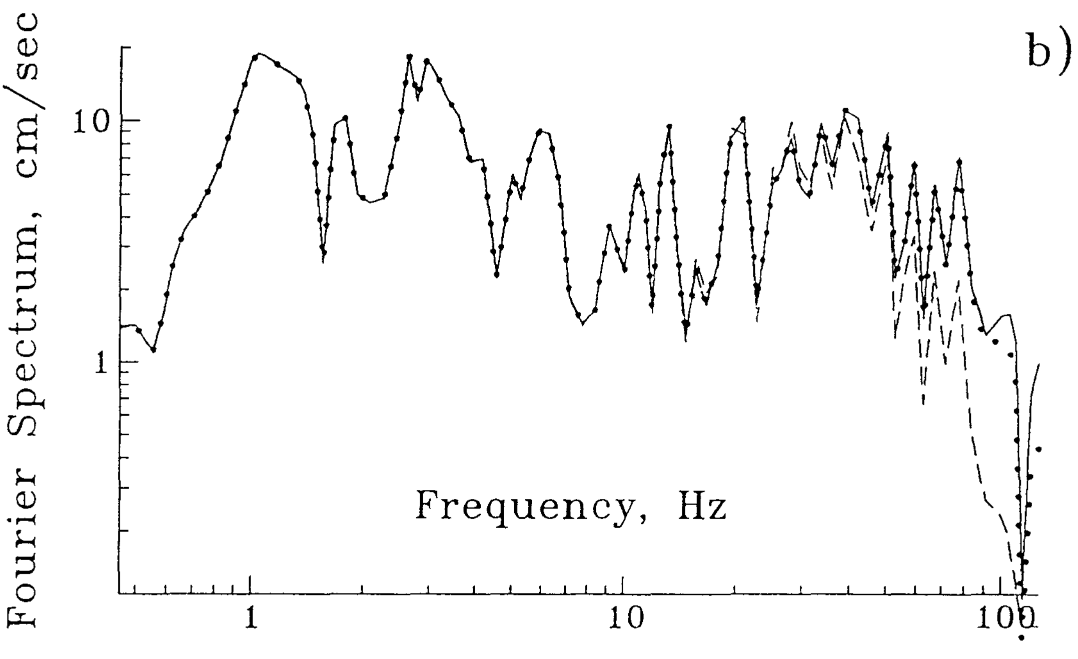

Figure 7. a) The ground acceleration time history: exact (solid line), appropriately scaled "recorded" (dashed line) and reconstructed by the proposed instrument correction procedure (dotted line). Exact and reconstructed time histories practically coincide. b) The Fourier spectra of the exact (solid line), "recorded" (dashed line) and reconstructed (dotted line) ground acceleration.

REFERENCES

Amini, A. and M.D. Trifunac (1985). Analysis of a Force Balance Accelerometer, Soil Dynamics and Earthquake Engineering, Vol. 4. No. 2, 82-90.

Amini, A. , O. Hata and M.D. Trifunac (1991). Experimental Analysis of RJL-1, Chinese Force Balance Accelerometer, Earthquake Engineering and Engineering Vibration, Vol. 11, No. 1, 77-88.

Cappellini, V., A.G. Constantinides and P. Emiliani (1978). Digital Filters and Their Applications, Academic Press Inc., (London).

Hamming, R.W. (1983). Digital Filters, Prentice-Hall, Englewood Cliffs, N.J.

Hudson, D.E. (1979). Unpublished Notes and Personal Communication.

Kojić, S., J.C. Anderson and M.D. Trifunac (1984). A Post Earthquake Response Analysis of the Imperial County Services Building, Dept. of Civil Eng. Rep. No. 84-02, Univ. of Southern California, Los Angeles, California.

Lee, V.W. and M.D. Trifunac (1979). Automatic Digitization and Processing of Strong Motion Accelerograms, Parts I and II, Department of Civil Engineering, Report No. 79-15 I and II, University of Southern California, Los Angeles, California.

Lee, V.W. and M.D. Trifunac (1984). Current Developments in Data Processing of Strong Motion Accelerograms, Department of Civil Engineering, Report No. 84-01, University of Southern California, Los Angeles, California.

Lee, V.W. and M.D. Trifunac (1987). Strong earthquake Ground Motion Data in EQINFOS: Part I, Department of Civil Engineering, Report No. 87-01, Univ. of Southern California, Los Angeles, California.

Neubert, H.K. (1975). Instrument Transducers: An Introduction to Their Performance and Design, Oxford, Clarendon Press, (2nd ed.).

Norton, H.N. (1969). Handbook of Transducers for Electronic Measuring Systems, Prentice Hall., Englewood Cliffs, N.J.,

Novikova, E.I. and M.D. Trifunac (1991). Instrument Correction for the Coupled Transducer-Galvanometer System, Department of Civil Engineering, Report No. 91-02, Univ. of Southern California, Los Angeles, California.

Oliver, F.J. (1971). Practical Instrumentation Transducers, Hayden Book Co., New York.

Trifunac, M.D. (1972). A Note on Correction of Strong-Motion Accelerograms for Instrument Response, Bull. Seism. Soc. of Amer., Vol. 62, pp. 401-409.

Trifunac, M.D. and V.W. Lee (1974). A Note on the Accuracy of Computed Ground Displacements from Strong-Motion Accelerograms, Bull. Seism. Soc. Amer., Vol. 64, 1209-1219.

Wong, H.L. and M.D. Trifunac (1977). Effects of Cross-Axis Sensitivity and Misalignment on Response of Mechanical Optical Accelerographs, Bull. Seism. Soc. Amer. Vol. 67, 929-956.